NASA TM-87054

AIAA'85

AIAA-85-1259

Wind Tunnel Results of Advanced High Speed Propellers in the Takeoff, Climb, and Landing Operating Regimes

George L. Stefko and Robert J. Jeracki, NASA Lewis Research Center, Cleveland, OH

AIAA/SAE/ASME/ASEE 21st Joint Propulsion Conference

July 8-10, 1985 / Monterey California

WIND TUNNEL RESULTS OF ADVANCED HIGH SPEED PROPELLERS IN THE TAKEOFF, CLIMB, AND LANDING OPERATING REGIMES

George L. Stefko and Robert J. Jeracki
National Aeronautics and Space Administration
Lewis Research Center
Cleveland, Ohio 44135

Abstract

Low speed wind tunnel performance tests of two advanced propellers have been completed at the NASA Lewis Research Center as part of the NASA Advanced Turboprop Program. The 62.2 cm (24.5 in) diameter adjustable pitch models were tested at Mach numbers typical of takeoff, initial climbout, and landing speeds (i.e., from 0.10 to 0.34) in the NASA Lewis 10- by 10-Foot Supersonic Wind Tunnel.

Both models had eight blades and a cruise design point operating condition of 0.80 Mach number, 10.668 km (35 000 ft.) I.S.A. altitude, 243.8 m/s (800 ft/sec) tip speed and a high power loading of 301 kW/m^2 (37.5 shp/ft^2).

No adverse or unusual low speed operating conditions were found during the test with either the straight blade SR-2 or the 45° swept SR-3 propellers. The 45° swept propeller efficiency exceeded the straight blade efficiency by 4 to 5 percent. Typical net efficiencies of the straight and 45° swept propeller at a Mach 0.20 takeoff condition were 50.2 and 54.9 percent respectively. At a Mach 0.34 climb condition, the efficiencies were 53.7 and 59.1 percent. Reverse thrust data indicated that these propellers are capable of producing more reverse thrust at Mach 0.20 than a high-bypass turbofan engine at Mach 0.20.

Introduction

The attractiveness of advanced turboprop propulsion results from its potential for very high propulsive efficiency at cruise speeds up to Mach 0.8. A comparison of the installed cruise efficiency of turboprop-powered and turbofan-powered propulsive systems is shown in Fig. 1 over a range of cruise speeds. The efficiencies shown in the figure include the installation losses for both systems; namely, nacelle drag for the turboprop systems, and fan cowling external drag and internal fan airflow losses associated with inlet recovery and nozzle efficiency for the turbofan systems. Conventional lower speed turboprops such as the Electra have installed efficiency levels above 80 percent up to about Mach 0.5, but can suffer from rapid decreases in efficiency above this speed due to increasing propeller compressibility losses. These losses are primarily the result of relatively thick blades (5 to 7 percent at 75 percent radius) operating at high helical tip Mach numbers.

The advanced high-speed turboprop has the potential to delay these compressibility losses to a much higher cruise speed and achieve a relatively high performance to at least Mach 0.8 cruise. Although high bypass ratio turbofans exhibit their highest efficiency at cruise speeds near Mach 0.8, their performance would still be significantly below that of the advanced turboprops.

A number of studies have been conducted by both NASA and industry to evaluate the potential of advanced high-speed turboprop propulsion for both civil and military applications. Numerous references to specific studies and summary results are listed in Ref. 1. Installed efficiency levels similar to those shown in Fig. 1 for comparable technology advanced turboprops and turbofans were used in most of these studies. At Mach 0.8 the installed efficiency of turbofan systems would be about 65 percent compared to about 75 percent for the advanced turboprop. At lower cruise speeds, the efficiency advantage of the advanced turboprop would be even larger.

The block fuel savings shown in Fig. 2 as a function of trip stage length is a summary of the Ref. 1 studies. As shown in Fig. 2, block fuel savings are dependent on aircraft cruise speed and range. At the bottom of the band, associated with Mach 0.8 cruise, fuel savings range from about 15 to 25 percent for advanced turboprop aircraft compared to equivalent technology turbofan aircraft. The larger fuel savings occur at the shorter operating ranges where the mission is climb and descent dominated. Because of the lower operating speeds encountered during climb and descent, turboprops have an even larger performance advantage over the turbofans than they do at Mach 0.8 cruise conditions. In a similar manner, a larger fuel savings is possible at Mach 0.7 cruise (represented by the top of the band in fig. 2). At this lower cruise speed, fuel savings range from about 20 percent to near 30 percent. Even larger fuel savings may be possible by recovering the propeller swirl loss from these single-rotation turboprops. Counter-rotation and swirl recovery vanes are two promising concepts for recovering the swirl loss. In addition, advanced airfoils can also improve perfomance. All of these concepts are currently under study at NASA and in the industry.

In view of the attractive fuel savings potential of the advanced high-speed turboprop propulsion system, NASA Lewis Research Center has established the Advanced Turboprop Program. This major research and technology program[2] establishes the technology base required to lead to the application of the advanced turboprop propulsion system concept. One phase of this overall program was to establish the complete low speed aerodynamic performance of the SR-2 and SR-3 propeller models in the takeoff, initial climbout, and landing speed regimes. The first model shown mounted in the wind tunnel (Fig. 3) had straight blades while the second model (Fig. 4) had 45° of blade sweep for lower noise and improved propeller efficiency. Both propeller models were tested in the NASA Lewis 10- by 10-Foot Supersonic Wind Tunnel on the Lewis Propeller Test Rig (PTR). This paper presents the wind tunnel test results of these two propellers in the takeoff, climb, and landing speed regime (i.e., Mach 0.10 to 0.34). Other wind tunnel tests have measured the performance of these propellers

primarily in the higher speed regime of Mach 0.60 to 0.85.[1,3]

Aerodynamic Design Concepts and Model Description

To achieve the previously described fuel savings, the propeller on the advanced turboprop would have to incorporate a number of unique design features that would enhance propeller performance and lower source noise. These unique design features are required to reduce blade compressibility losses and attain high efficiency in the transonic Mach number regime. A propeller designed for a cruise Mach number of 0.80 at an altitude above 9.144 km (30 000 ft), would have local blade Mach numbers from just over 0.8 at the blade hub to supersonic Mach numbers (near 1.15) at the blade tip. The inherent detrimental effects of these high Mach numbers on performance are negated by the design concepts shown in Fig. 5. These concepts include proper shaping of the nacelle to reduce inboard blade Mach number, blade sweep to reduce outboard blade local Mach number, thinner blades to increase drag rise Mach number and spinner area ruling to prevent in-board blade choking. To hold propeller diameter to a reasonable value, a high power (or disk) loading and concomitantly a large number of blades (8 or 10) and increased chord length are required. The inboard portion of the propeller then operates as a cascade rather than isolated blades. These design concepts are incorporated in the two model propellers.

The propeller models (Figs. 3 and 4) were both designed for an operating condition of 0.80 Mach number, 10.668 km (35 000 ft) I.S.A. altitude, 243.8 m/s (800 ft/sec) tip speed and a power loading of 301 kW/m^2 (37.5 shp/ft^2). Both models have a diameter of 0.622 m (24.5 in) which was determined by the design power loading. The overall design characteristics and planforms of the two models are presented in Table 1.

The aerodynamic conic-corrected blade shape characteristics along mean flow streamlines are presented for the SR-2 propeller in Fig. 6 and the 45° swept SR-3 propeller in Fig. 7. The thickness ratio (t/b), twist ($\Delta\beta$), design lift coefficient (C_{L_D}) and planform (b/D) distributions were established to provide a loading distribution at the design condition for high efficiency and for the SR-3 propeller, low noise.

The airfoil sections selected for the SR-2 and SR-3 blade design are NACA Series 16 from the tip to the 45 and 53 percent radius respectively, and NACA Series 65 with circular arc (CA) camber lines from the 37 percent radius to the root with a transition fairing between. These airfoils were chosen for their high critical Mach number and wide, low drag buckets.

The area ruled spinners and nacelle lines are designed to alleviate blade root choking and minimize compressibility drag rise. The spinners incorporate area-ruling and blend into the nacelle. The nacelle has a maximum diameter equal to 35 percent of the model propeller diameter.

The performance data were acquired for a model configuration which had the gaps between the propeller blade roots and the hub surface sealed. The gaps were disproportionately large for the model and were sealed to be more representative of a full scale propeller. More design information may be found in Refs. 1[4], 3-5.

Wind Tunnel Test Program

Wind Tunnel

The SR-2 and SR-3 propeller model tests were conducted in the NASA Lewis 10- by 10-Foot Supersonic Wind Tunnel. This tunnel[5] incorporates a 13.12 m (40 ft) long, solid wall test section. Nominal test section Mach numbers can vary subsonically from 0.10 to 0.34 and supersonically from 2.0 to 3.5. The tunnel was run in the aerodynamic cycle versus the propulsion cycle for this test program. During the aerodynamic cycle, the tunnel is operated as a closed system with make-up air added only as required to maintain the desired tunnel conditions. The freestream velocity corrections due to the propeller thrust in this solid wall tunnel are discussed in detail in Appendix B of Ref. 5.

Propeller Test Rig (PTR)

The 746 kW (1000 hp) PTR was designed and developed specifically for conducting research on advanced propellers in the Lewis 10- by 10-foot and 8- by 6-foot wind tunnels. The PTR was strut-mounted from the ceiling in the tunnel test section. The PTR and the SR-3 model are shown in the tunnel (Fig. 4) while a cutaway view of the PTR is presented in Fig. 8. The model is driven by a three-stage air turbine utilizing high pressure air at 3.1×10^6 N/m^2 (450 psi) and heated to 367 K (660 °R). The turbine is capable of delivering nearly 746 kW (1000 hp) to the propeller model.

The PTR metric system includes two separate axial force measuring systems. The primary system is a rotating balance which measures thrust and torque of the propeller and spinner. The second system includes a load cell located in the vertical strut. Both systems measure propeller blade and spinner forces only, when corrected for internal pressure tares. Model parts, other than the spinner and blades, that are metric to the strut mounted load cell are shielded from the freestream tunnel air by a windscreen (Fig. 8).

Extensive static calibrations of the load cell and rotating balance were done. Limited dynamic thrust calibrations were also done. The dynamic torque calibrations could only be done with zero torque. All these calibrations were performed before, during, and after the tests to assure that no changes occurred during the test. The calibrations are discussed in more detail in Ref. 5.

Determination of the Propeller Net Force

The net propeller thrust is defined as the propulsive force of the blades operating in the presence of the spinner and nacelle flow field without the increase in thrust (i.e., apparent thrust) due to the mutual interaction between the propeller blades, the spinner and the nacelle.

To determine the difference between apparent and net thrust, model tare tests were made first

without the propeller blades to evaluate both the external spinner aerodynamic drag and the nacelle pressure drag.

In these tare tests the spinner was replaced by a "dummy" hub having no holes for the blades. A special series of experimental runs was made to define the spinner aerodynamic and nacelle pressure drag for the same range of tunnel Mach numbers as would be tested with the model blades. As shown in Fig. 9(a), the spinner drag (D_{ST}) was measured directly from the force balance and corrected for the internal pressure area forces. The nacelle pressure drag (D_{NT}), was determined by pressure integration of the longitudinal rows of area-weighted pressure orifices.

With the propeller blades installed and thrusting, the force balance measures the algebraic sum of the propeller thrust, the spinner drag, and the internal pressure area forces. The model forces are as shown in Fig. 9(b). The uncorrected propeller thrust (T_{PROP} in Fig. 9(b)) is defined as:

$$T_{PROP} = FB - \sum PA_{INT} + D_S$$

When this uncorrected propeller thrust is corrected for the change in spinner drag (ΔD_S) between the powered data (Fig. 9(b)) and the tare data (Fig. 9(a));

$$\Delta D_S = D_S - D_{ST}$$

the apparent thrust of the propeller is obtained from:

$$T_{APP} = T_{PROP} - \Delta D_S$$

or

$$T_{APP} = FB - \sum PA_{INT} + D_{ST}$$

where

$$PA_{INT} = (p - p_o)\, A_{INT}$$

Now, the nacelle pressure drag was obtained from nacelle surface pressure integrations:

$$D_N = \int (p - p_o)\, dA$$

The change in nacelle pressure drag, ΔD_N, was obtained from the difference between these and the tare run pressure integrations:

$$\Delta D_N = D_N - D_{NT}$$

And finally, the net thrust was obtained by subtracting the change in nacelle pressure drag from the apparent thrust:

$$T_{NET} = T_{APP} - \Delta D_N$$

More information on the propeller test procedures used in this test may be found in Ref. 5.

Test Results

Takeoff, Climb and Landing Performance

The SR-2 and SR-3 propeller models were tested at zero angle of attack over a range of Mach numbers from 0.10 to 0.34 and blade angles from -6.8° to 62.1°. The blade angle ($\beta_{0.75R}$), measured at 75 percent of the propeller radius, becomes 90° when the chord of that airfoil section is aligned directly with the flight direction. At each blade angle, model thrust and power were measured over a range of Mach numbers and rotational speeds. The blade angle/Mach number combinations tested are listed in Table 2 for the SR-2 propeller and Table 3 for the SR-3 propeller. At each blade angle/Mach number combination, measurements were taken over an rpm range from the windmilling value to 9000 rpm, the maximum rpm allowed by blade stress limitations. Each rotational speed setting constituted a test point.

The SR-2 and SR-3 propeller performance is summarized in Figs. 10 to 17 for freestream Mach numbers of 0.10, 0.20, 0.27, and 0.34. These propeller performance efficiency maps present the propeller net efficiency (η_{NET}) and reference power coefficient ($C_{P_{REF}}$) for a given advance ratio (J_{REF}) and blade angle. The reference power coefficients and the advance ratios are based upon the propeller reference diameter of 62.2 cm (24.5 in). This reference designation is used because the actual true tip diameter for the swept SR-3 propeller changes with blade angle and rotational speed as shown in Fig. 18. Reference power coefficient and reference advance ratio are defined as:

$$C_{P_{REF}} = \frac{P}{\rho_o n^3 D_{REF}^5}$$

$$J_{REF} = \frac{V_o}{n\, D_{REF}}$$

In these figures the performance of the propeller is expressed as net efficiency which corresponds to the net propulsive thrust produced with the propeller operating in the velocity field of the nacelle and spinner. Net efficiency is defined as:

$$\eta_{NET} = \frac{\text{Net Thrust x Freestream Velocity}}{\text{Shaft Power}}$$

and, in dimensionless form:

$$\eta_{NET} = \frac{C_{T_{NET}} J}{C_P} \quad \text{or} = \frac{C_{T_{NET,REF}} J_{REF}}{C_P}$$

where

$$C_{T_{NET,REF}} = \frac{T_{NET}}{\rho_o n^2 D_{REF}^4}$$

During the thorough testing in the low speed operating envelope, no adverse operating conditions were found. Nor, were any areas of significant propeller performance loss found that might be indictive of separated flow on the propeller airfoils.

Some comparisons of the performance of the straight blade SR-2 propeller versus the 45° swept SR-3 propeller at four low speed operating conditions can be made.

When the airplane is accelerating down the runway, a representative condition would be a Mach number of 0.10, an advance ratio of 0.438, and a power coefficient of 0.50. At this condition, the 45° swept SR-3 propeller design had an efficiency of 43.5 versus 38.6 percent for the straight SR-2 propeller design, a 4.9 percent advantage.

Near the airplane's liftoff condition, the Mach number would be around 0.20, the advance ratio at 0.875, and the power coefficient at 1.00. At this condition, the swept SR-3 propeller has a net efficiency of 54.9 versus 50.2 percent for the SR-2 propeller, a 4.7 percent advantage.

When the airplane is starting its initial climbout, a typical operating condition is a Mach number of 0.27, an advance ratio of 1.16, and a power coefficient of 1.37. Again, the 45° swept SR-3 propeller net efficiency is significantly higher than the SR-2 propeller net efficiency with a value of 57.2 versus 52.9 percent, a 4.3 percent advantage.

And finally, when the airplane is farther into its climbout, a representative condition would be a Mach number of 0.34, an advance ratio of 1.40 and a power coefficient of 1.70. At this condition, the 45° swept SR-3 propeller net efficiency is 59.1 versus 53.7 percent for the straight SR-2 propeller, a 5.4 percent advantage.

Thus, the measured data show that in the low speed operating regime, the 45° swept SR-3 propeller net efficiency exceeded the net efficiency of the straight bladed SR-2 propeller by about 4 to 5 percent. The SR-3 performance improvement over the SR-2 performance is due to a combination of design factors such as more blade sweep, a better twist, chord and lift distribution, and a better spinner and area-ruled hub design.

Reverse Thrust Performance

In view of the importance of reverse thrust capability of the propulsion system on transport aircraft, the reverse thrust characteristics of the 45° swept SR-3 propeller were investigated at 0.10 and 0.20 Mach numbers. The blade angle was set at -6.8°. Due to mechanical interference, this was the maximum reverse blade angle that could be achieved with the model Prop-Fan. The test results are presented in Fig. 19 in terms of power and thrust coefficients as a function of advance ratio. In Fig. 20, the reverse thrust is divided by the takeoff thrust at Mach 0.20. This parameter is presented versus velocity for the windmilling and powered SR-3 propeller. For reference, a high-bypass turbofan engine is also shown on this figure. The curves show that the powered SR-3 propeller produce more reverse thrust than that of a high-bypass turbofan engine. Thus, the advanced SR-3 eight-bladed propeller is capable of producing the large breaking forces desired for transport airplanes.

Summary of Results

Two variable pitch advanced turboprop propeller models (the straight-bladed SR-2 and the 45° swept SR-3) were installed in the NASA Lewis 10- by 10-Foot Supersonic Wind Tunnel and performance tested at subsonic conditions corresponding to typical takeoff, initial climbout, and landing speeds. The following results were obtained:

1. No adverse operating conditions nor areas of significant propeller performance loss indicative of separated flow on the propeller airfoils were found in the low speed operating envelope (i.e, Mach 0.10 to 0.34) with either the straight bladed SR-2 or 45° swept SR-3 propellers.

2. The 45° swept propeller appeared to be better designed for low speed operation than the straight bladed SR-2 propeller because it was more efficient. The 45° SR-3 swept propeller net efficiency exceeded the efficiency of the straight bladed SR-2 propeller by about 4 to 5 percent at all low speed operating conditions. Two of the low speed operating conditions are summarized below:

(a) At the Mach 0.20 takeoff liftoff condition ($J = 0.875$ and $C_p = 1.0$), the straight bladed SR-2 propeller had a net efficiency of 50.2 percent while the 45° swept SR-3 propeller had a net efficiency of 54.9 percent. The swept SR-3 advantage was 4.7 percent.

(b) At a Mach 0.34 climbout condition ($J = 1.40$ and $C_p = 1.70$), the straight bladed SR-2 propeller had a net efficiency of 53.7 percent while the 45° swept SR-3 propeller had a net efficiency of 59.1 percent. The swept SR-3 advantage was 5.4 percent.

3. The large amount of reverse thrust measured for the SR-3 propeller indicates that these new propellers are capable of producing more reverse thrust than that of a high-bypass transport turbofan engine.

Appendix A - Symbol List

A	area, m^2
	blade activity factor, $6250\int_{(r/B)\text{ at hub}}^{1.0} (b/D)(r/R)^3\,dx$
b	elemental blade chord, m
CA	circular arc
C_{LD}	blade design lift coefficient
C_{Li}	integrated design lift coefficient, $4\int_{(r/B)\text{ at hub}}^{1.0} C_{LD}(r/R)^3\,dx$
C_P	power coefficient = $P/\rho_0 n^3 D^5$
C_T	thrust coefficient = $T/\rho_0 n^2 D^4$
D	propeller diameter, m
D_N	nacelle drag, N
D_{NT}	nacelle tare drag, N

D_S	spinner drag, N
D_{ST}	spinner tare drag, N
dA	elemental area, m^2
FB	force balance, N
J	advance ratio = V_o/nD
M	Mach number
n	rotational speed, rps
P	power, W
PA	pressure forces in the form $(p - p_o) \cdot$ Area, N
p	pressure, N/m^2
R	propeller radius, m
r	radius, m
r/R	fractional radius
T	thrust, N
T_{PROP}	uncorrected propeller thrust, N
t	elemental blade maximum thickness, m
V	velocity, m/sec
β	blade angle, deg
$\Delta\beta$	change in blade angle from the angle at the 75 percent blade radius, deg
$\beta_{0.75R}$	static propeller blade angle at 75 percent blade radius, deg
η	efficiency in percent = $TV_o/P \cdot 100$
ρ	mass density, kg/m^3

Subscripts

APP	apparent
INT	internal
N	nacelle
o	tunnel freestream condition
REF	reference, based upon 62.2 cm (24.5 in) reference diameter
T	tare

References

1. Jeracki, R.J., Mikkelson, D.C., and Blaha, B.J., "Wind Tunnel Performance of Four Energy Efficient Propellers Designed for Mach 0.8 Cruise," SAE Paper 790573, Apr. 1979.

2. Whitlow, J.B., Jr., and Sievers, G.K., "Fuel Savings Potential of the NASA Advanced Turboprop Program," NASA TM-X-83736, 1984.

3. Rohrbach, C., Metzger, F.B., Black, D.M., and Ladden, R.M., "Evaluation of Wind Tunnel Performance Testing of an Advanced 45° Swept Eight-Bladed Propeller at Mach Numbers from 0.45 to 0.85," NASA CR-3505, 1982.

4. Mikkelson, D.C., Blaha, B.J., Mitchell, G.A., and Wikete, J.E., "Design and Performance of Energy Efficient Propellers for Mach 0.8 Cruise," SAE Paper 770458, Mar. 1977.

5. Stefko, G.L., and Jeracki, R.J., "Wind Tunnel Results of Advanced High Speed Propellers at Takeoff, Climb, and Landing Mach Numbers", NASA TM-87030, August, 1985.

6. Aiello, R.A., "NASA Lewis 10- by 10-Foot Supersonic Wind Tunnel," NASA TM-X-71625, 1974.

TABLE 1. - DESIGN CHARACTERISTICS AND PLANFORMS OF THE SR-2 AND SR-3 MODEL PROPELLERS

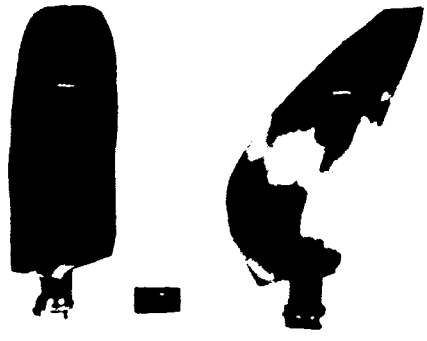

	SR-2	SR-3
Number of blades	8	8
Tip sweep angle, deg	0	45
Model diameter, cm (in)	62.2 (24.5)	62.2 (24.5)
Tip speed, m/sec (ft/sec)	244 (800)	244 (800)
Power loading, kW/m^2 (shp/ft^2)	301 (37.5)	01 (37.5)
Activity factor	203	235
Integrated design lift coefficient	0.081	0.214
Airfoils	NACA 16 and 65/CA	NACA 16 and 65/CA
Ratio of nacelle maximum diameter to propeller diameter	0.35	0.35
Cruise design Mach number	0.80	0.80
Cruise design advance ratio	3.06	3.06
Cruise design power coefficient	1.7	1.7
Measured cruise design net efficiency, %	76	78
Measured cruise noise level, dB	151	146

TABLE 2. - SR-2 PROPELLER TEST RUN SCHEDULE

Blade angle at 75 percent radius, deg	Mach number			
	0.10	0.20	0.27	0.34
24.9	X	X	-	-
29.6	X	X	-	-
34.4	X	X	X	-
38.0	X	X	X	-
41.7	X	X	X	X
45.8	-	X	X	X
49.8	-	X	X	X
53.8	-	-	X	X
59.7	-	-	X	X

TABLE 3. - SR-3 PROPELLER TEST RUN SCHEDULE

Blade angle at 75 percent radius, deg	Mach number				
	0.00	0.10	0.20	0.27	0.34
-6.8	X	X	X	-	-
24.6	-	X	X	-	-
29.4	-	X	X	-	-
33.9	-	X	X	X	-
37.3	-	X	X	X	-
41.9	-	X	X	X	-
45.9	-	X	X	X	X
48.3	-	-	X	X	X
51.4	-	-	X	X	X
54.1	-	-	X	X	X
58.3	-	-	X	X	X
62.1	-	-	-	X	X

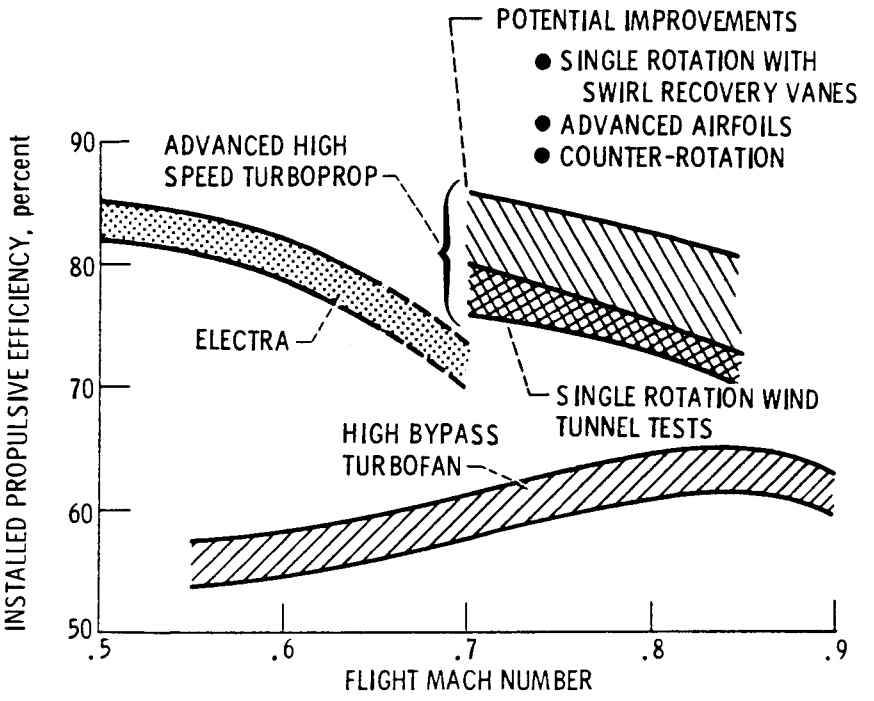

Figure 1. - Installed propulsive efficiency trends of advanced turboprops compared to equivalent technology turbofans.

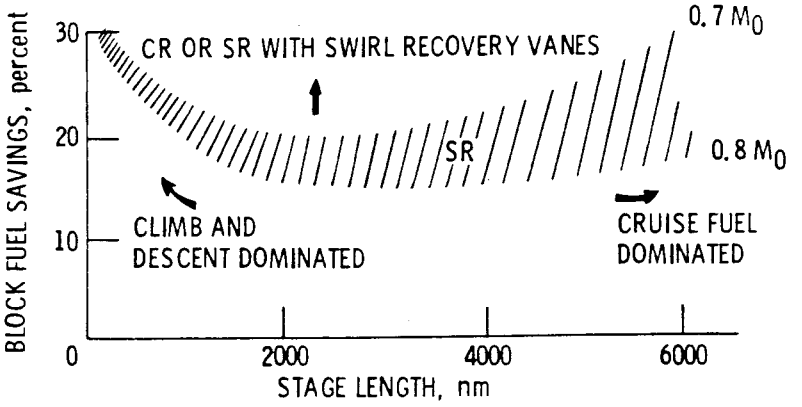

Figure 2. - Fuel savings trends of advanced turboprop aircraft over comparable turbofan aircraft.

Figure 3. - The SR-2 propeller model with straight blades installed in the NASA Lewis 10-by 10-Foot Supersonic Wind Tunnel.

Figure 4. - The SR-3 propeller model with 45 degree swept blades installed in the NASA Lewis 10-by 10-Foot Supersonic Wind Tunnel.

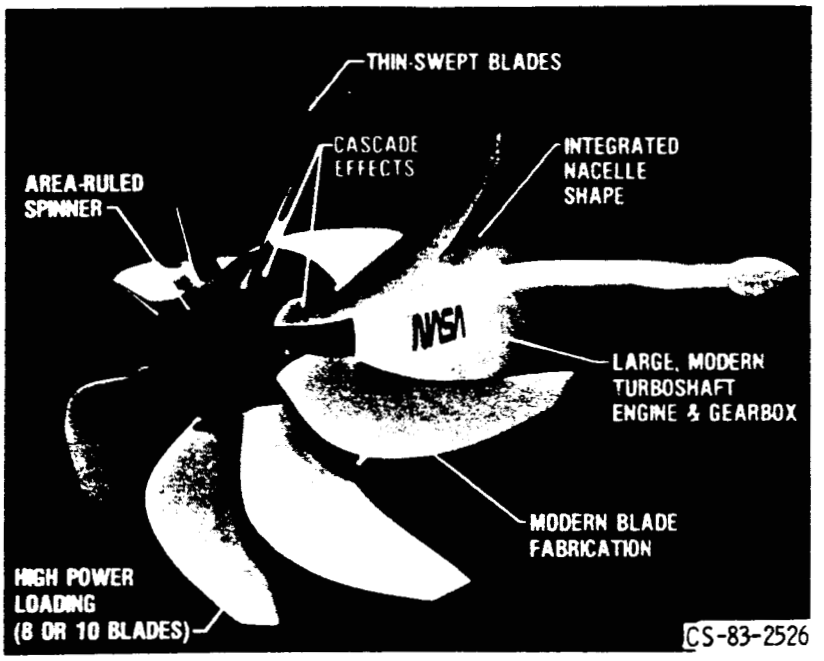

Figure 5. - Aerodynamic design concepts for an advanced high speed turboprop propulsion system.

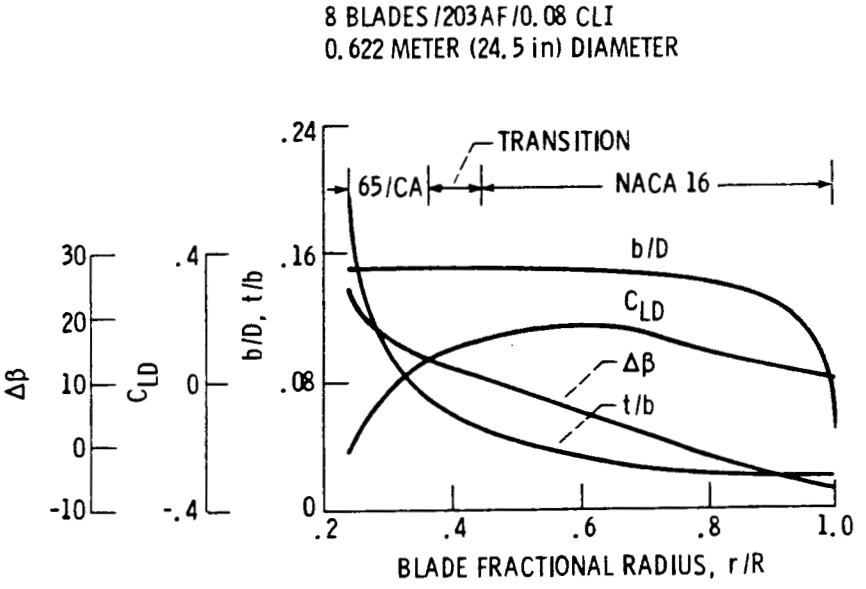

Figure 6. - Variation of propeller design parameters with blade radius for the unswept SR-2 propeller.

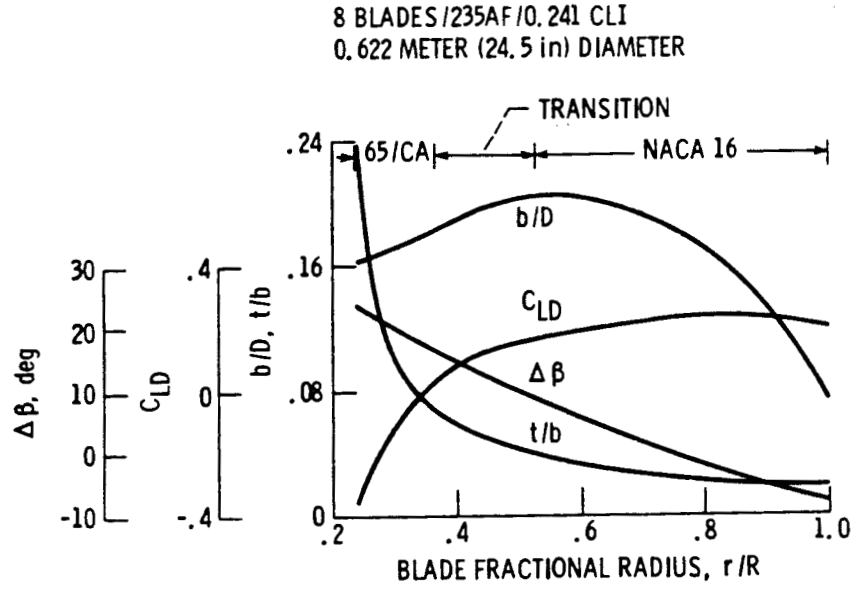

Figure 7. - Variation of propeller design parameters with blade radius for the 45 degree swept SR-3 propeller.

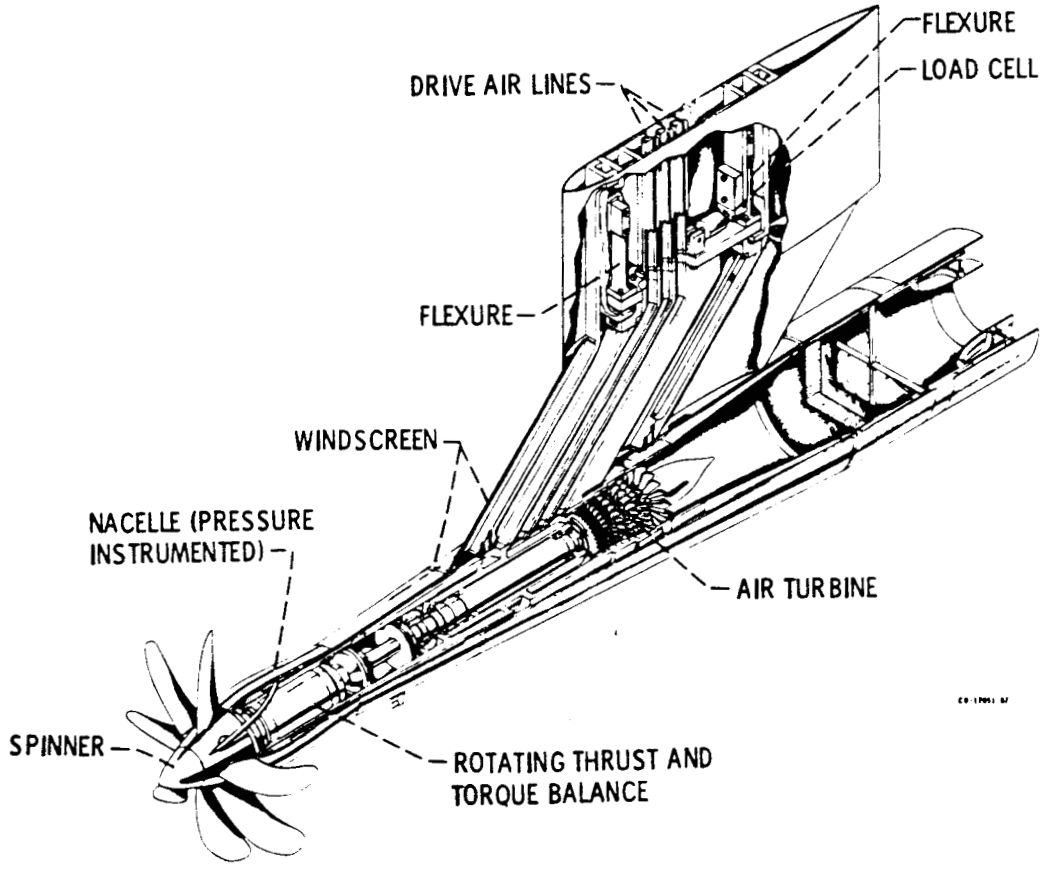

Figure 8. - Cutaway view of the Lewis 1000 horsepower (746 kW) propeller test rig.

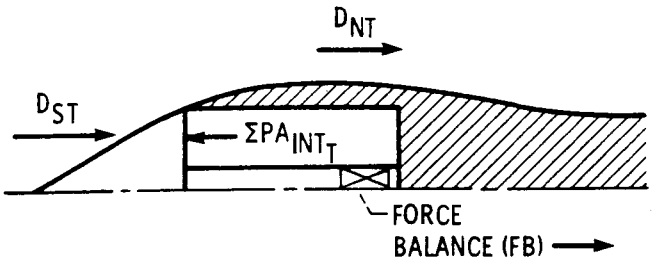

$$-D_{ST} = FB_T - \Sigma PA_{INT_T}$$

$$D_{NT} = (p_N - p_O)\, dA_N$$

(a) Forces acting on balance during tare runs.

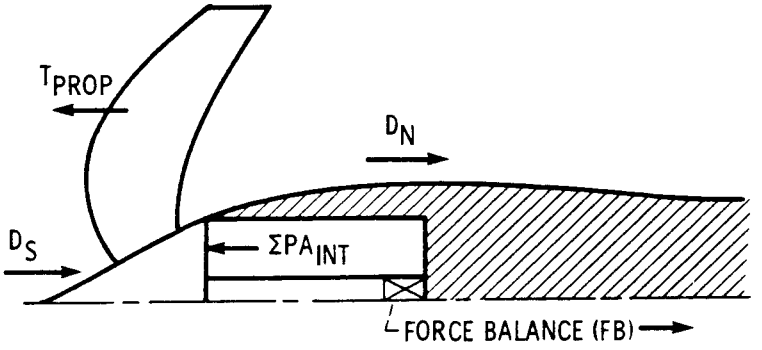

(b) Forces acting on balance during test runs.

Figure 9. - Forces acting on balance during tare and test runs.

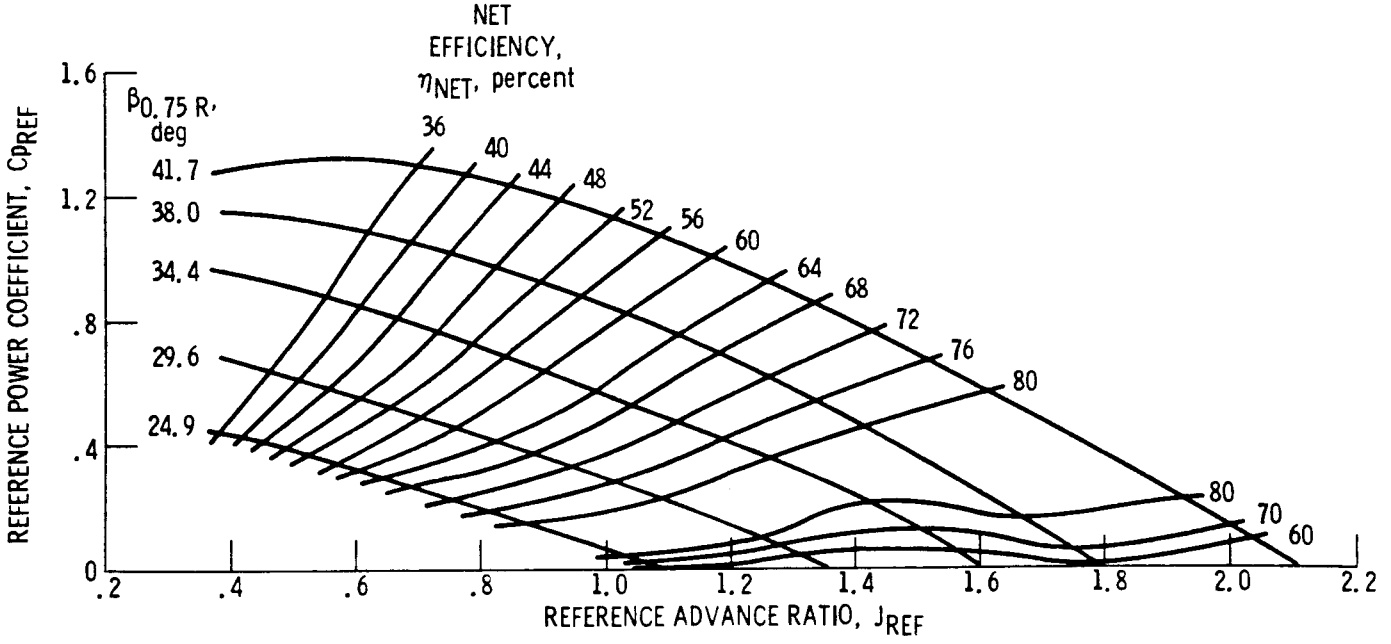

Figure 10. - SR-2 propeller efficiency map at a Mach number of 0.10.

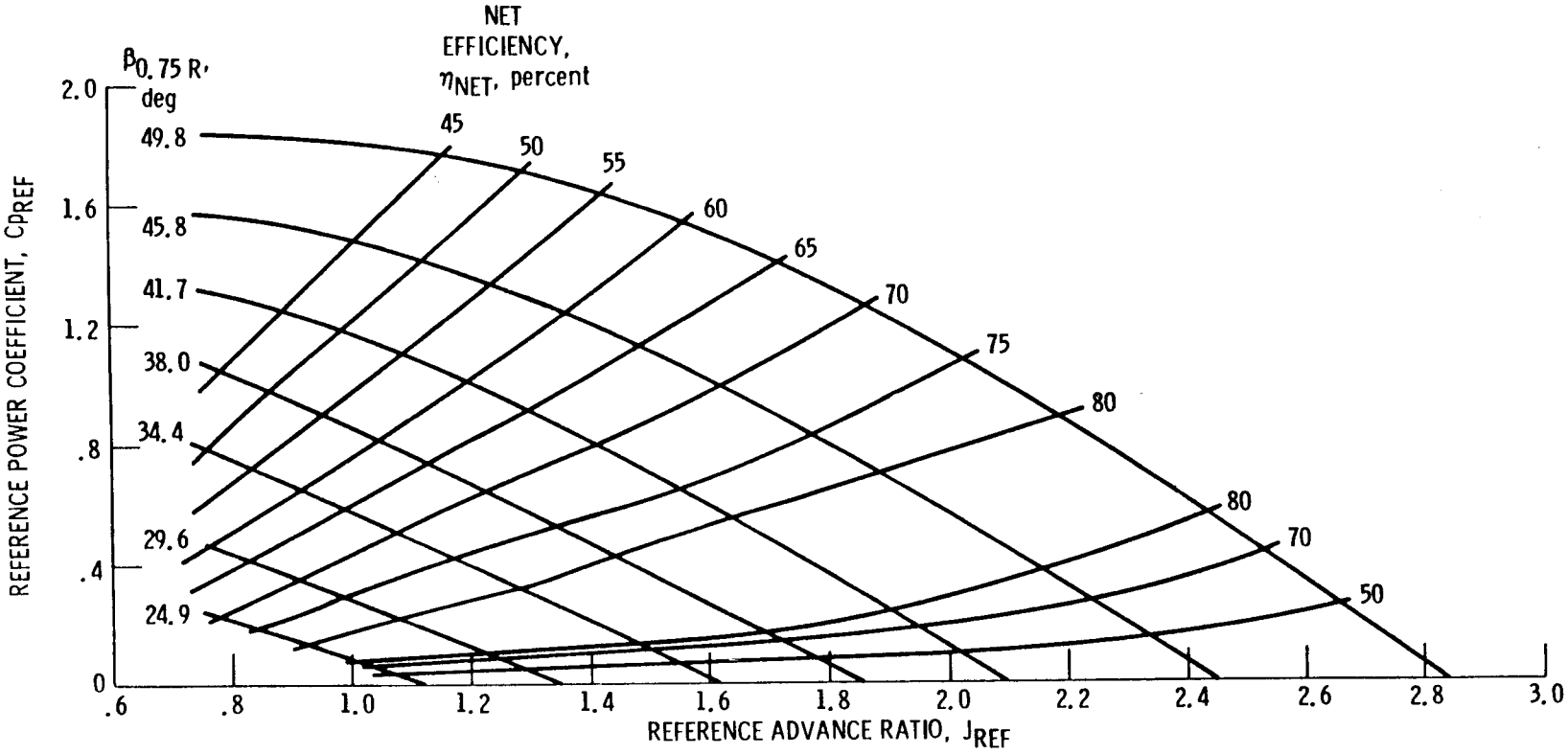

Figure 11. - SR-2 propeller efficiency map at a Mach number of 0.20.

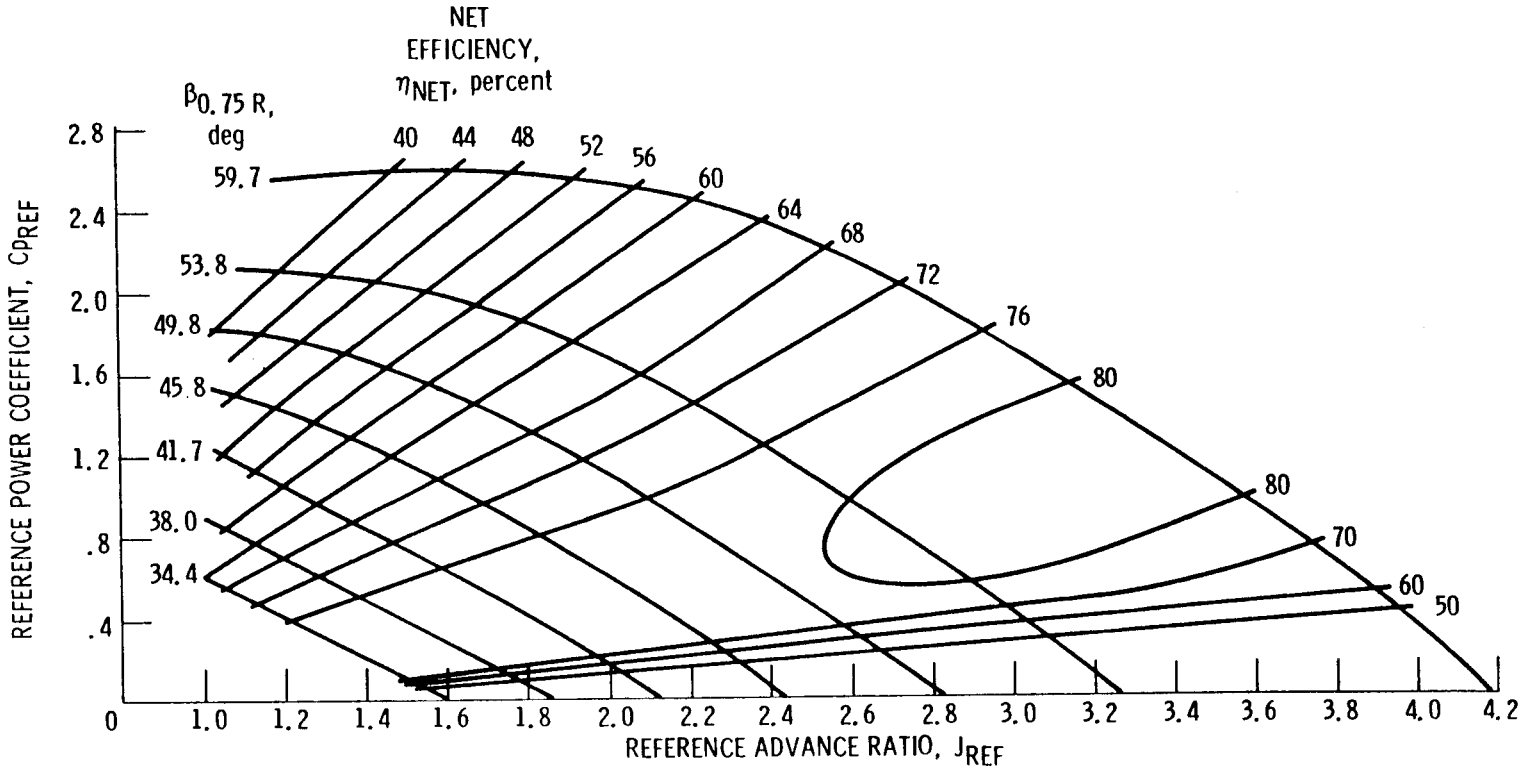

Figure 12. - SR-2 propeller efficiency map at a Mach number of 0.27.

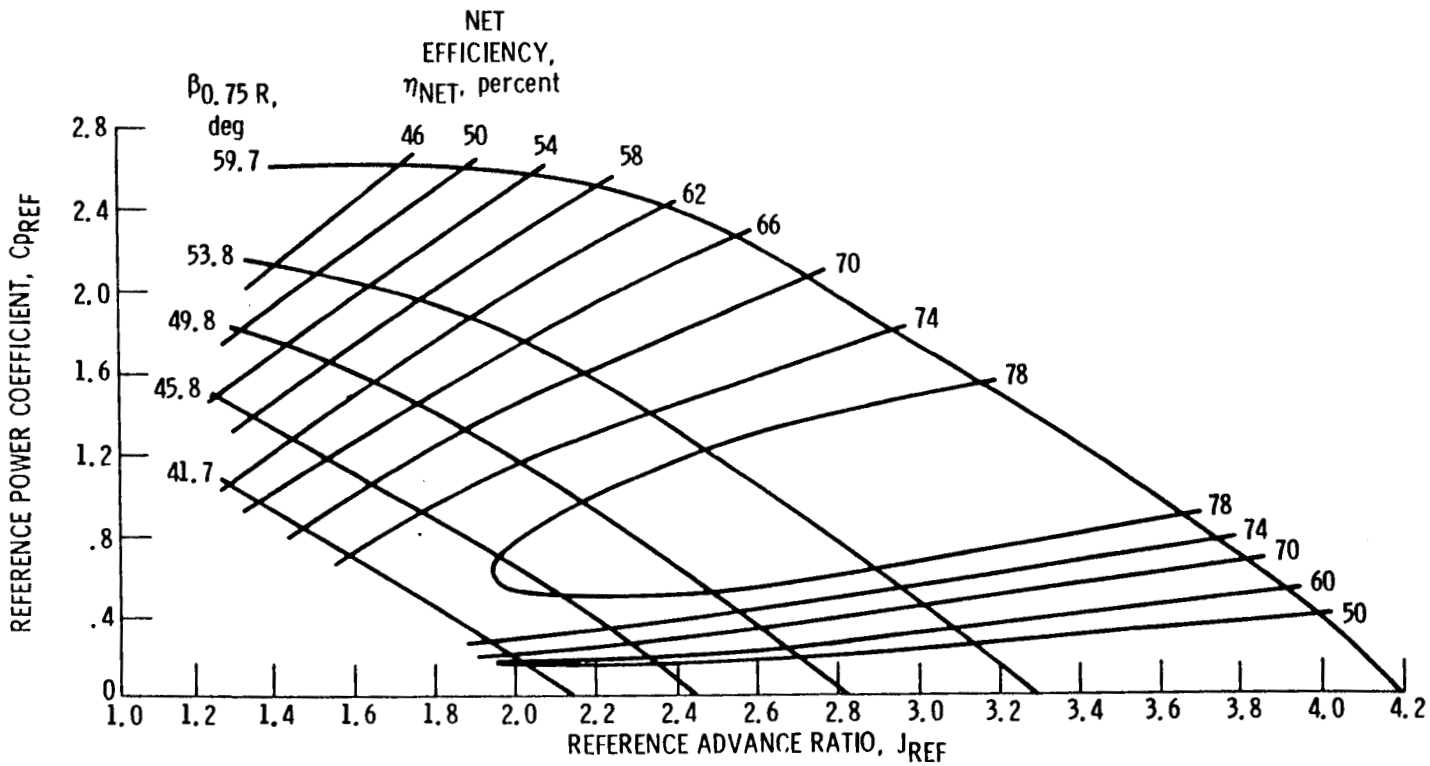

Figure 13. - SR-2 propeller efficiency map at a Mach number of 0.34.

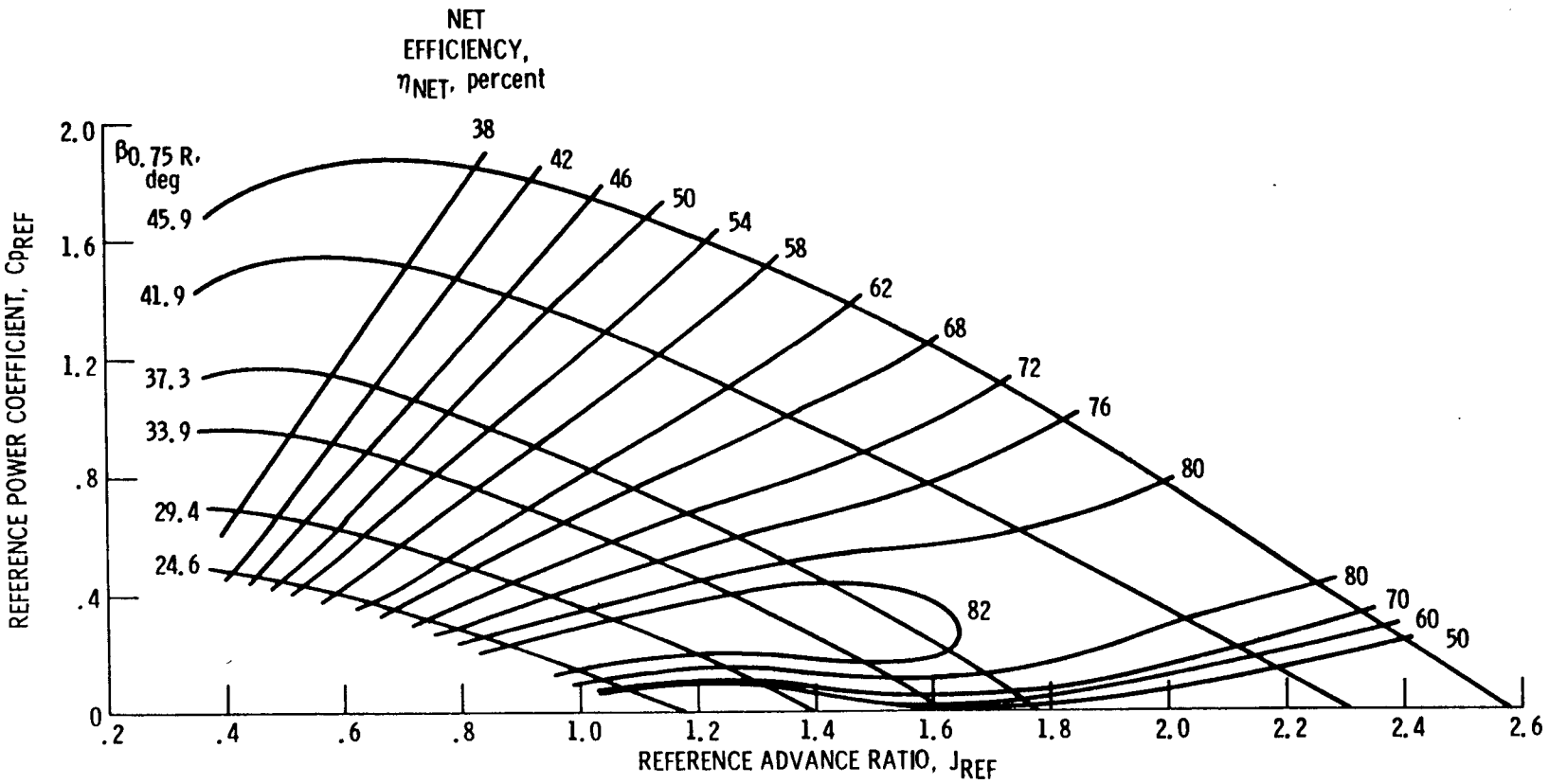

Figure 14. - SR-3 propeller efficiency map at a Mach number of 0.10.

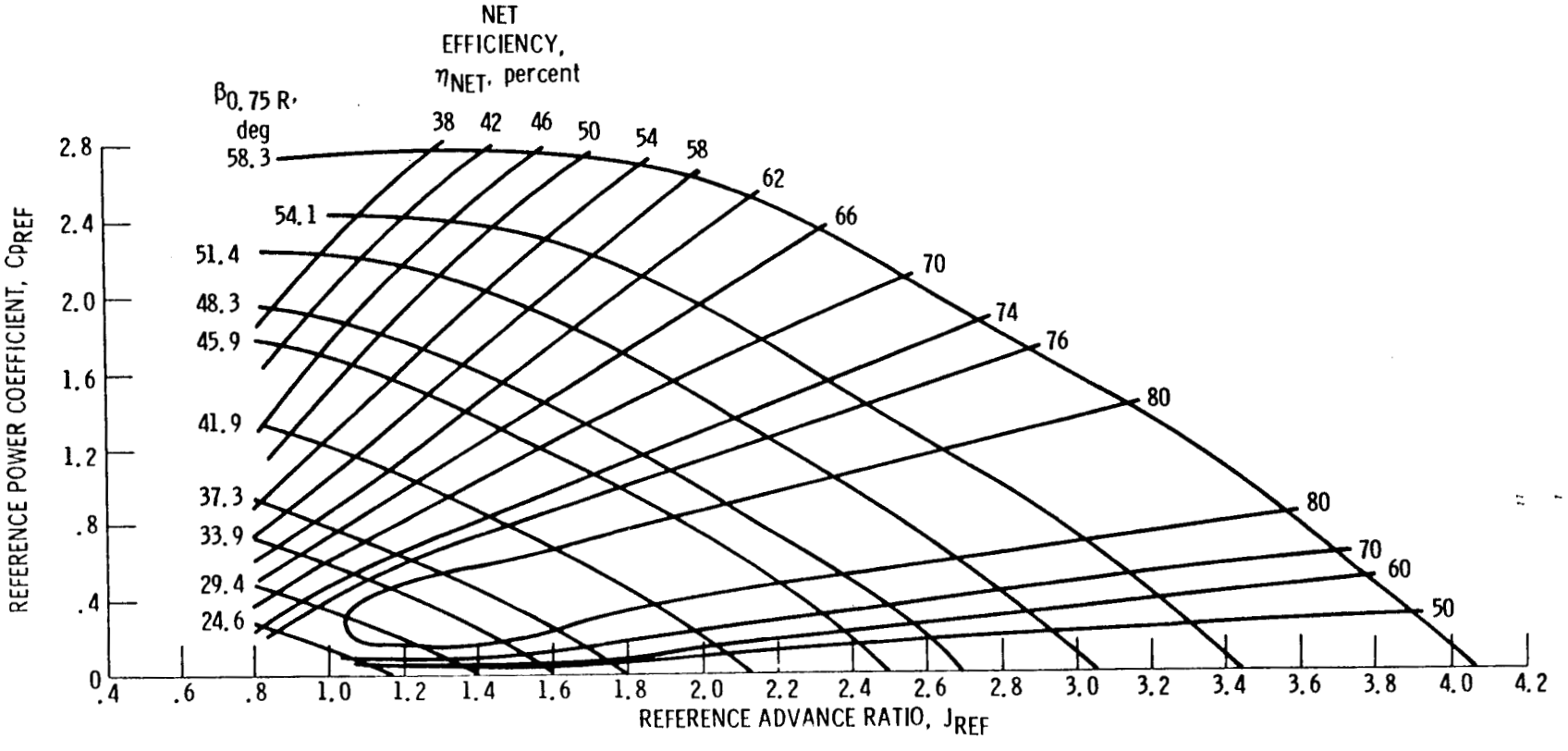

Figure 15. - SR-3 propeller efficience map at a Mach number of 0.20.

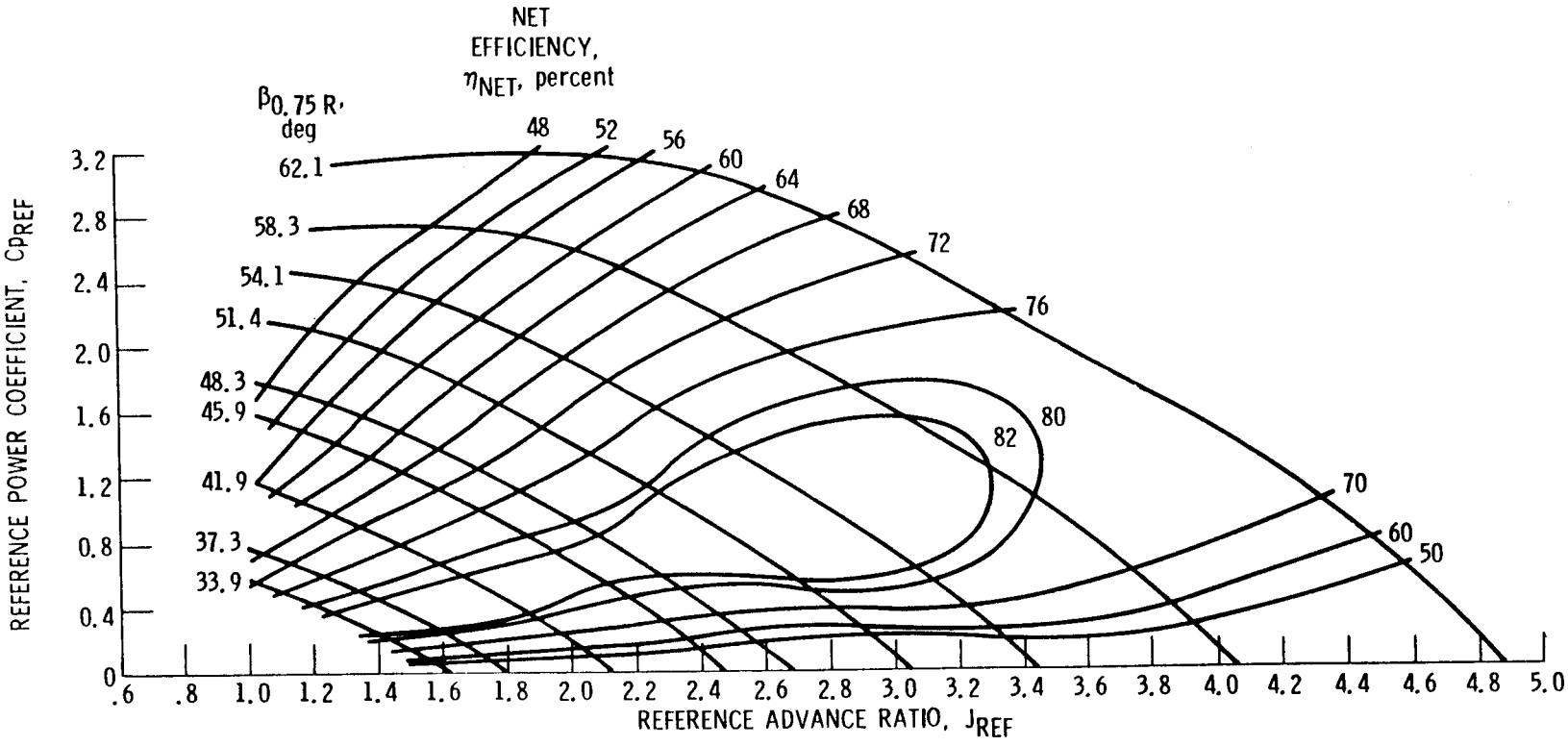

Figure 16. - SR-3 propeller efficiency map at a Mach number of 0.27.

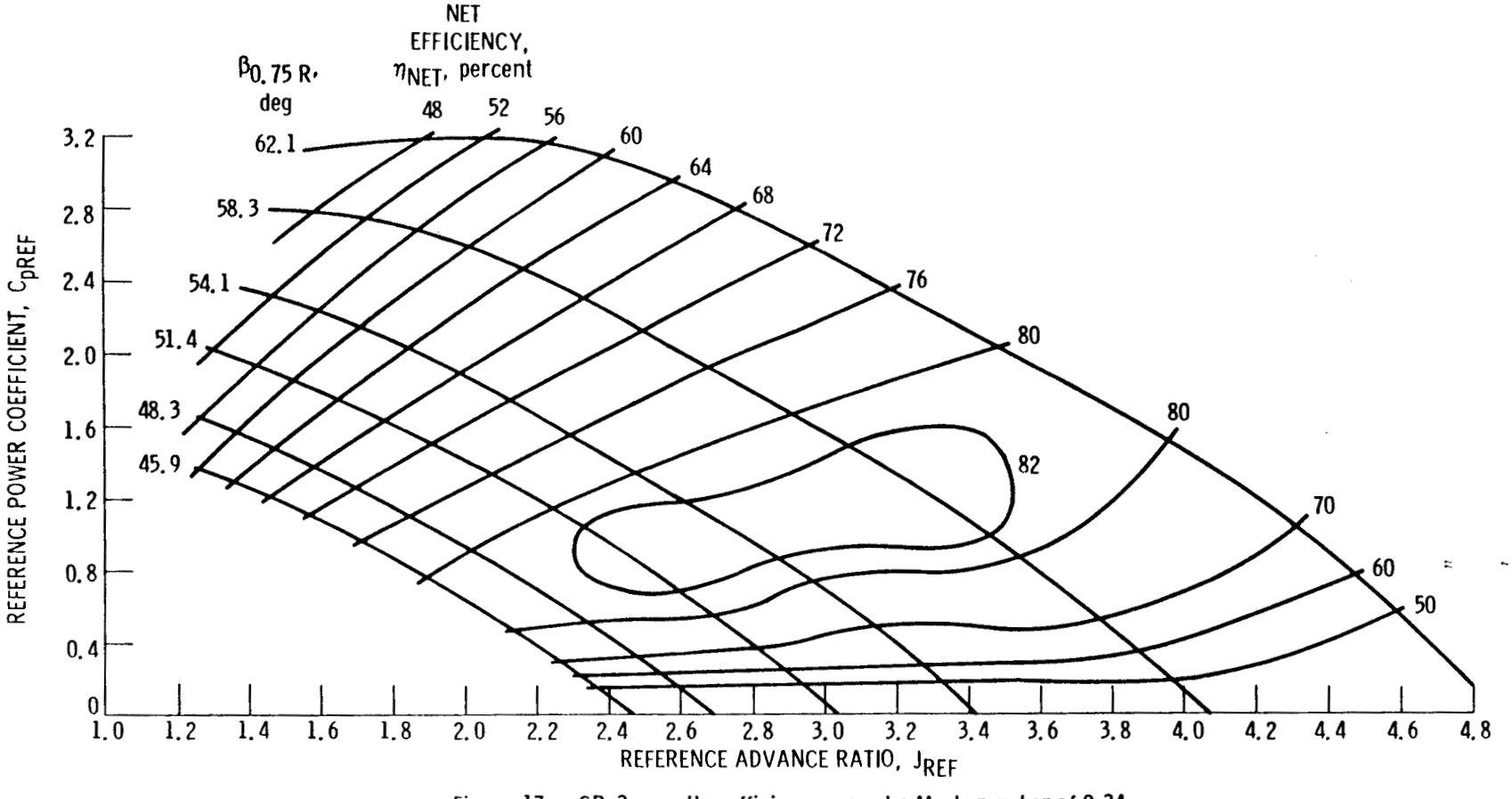

Figure 17. - SR-3 propeller efficiency map at a Mach number of 0.34.

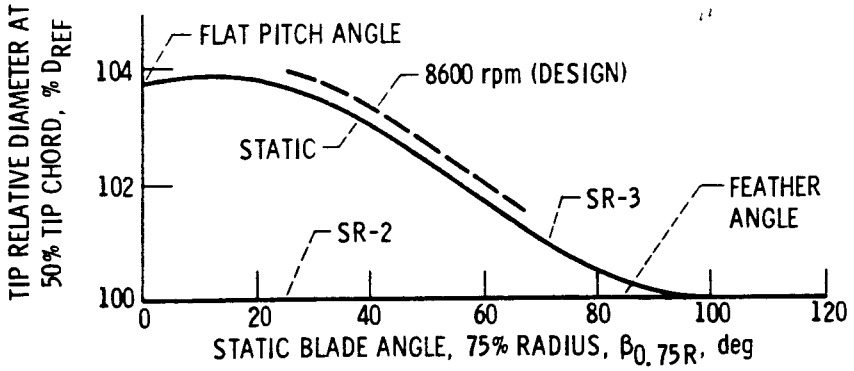

Figure 18. - Variation of tip relative diameter with blade angle and rotation speed. D_{REF} = 62.23 cm (24.5 in); $\beta_{0.75R}$ = 102^0.

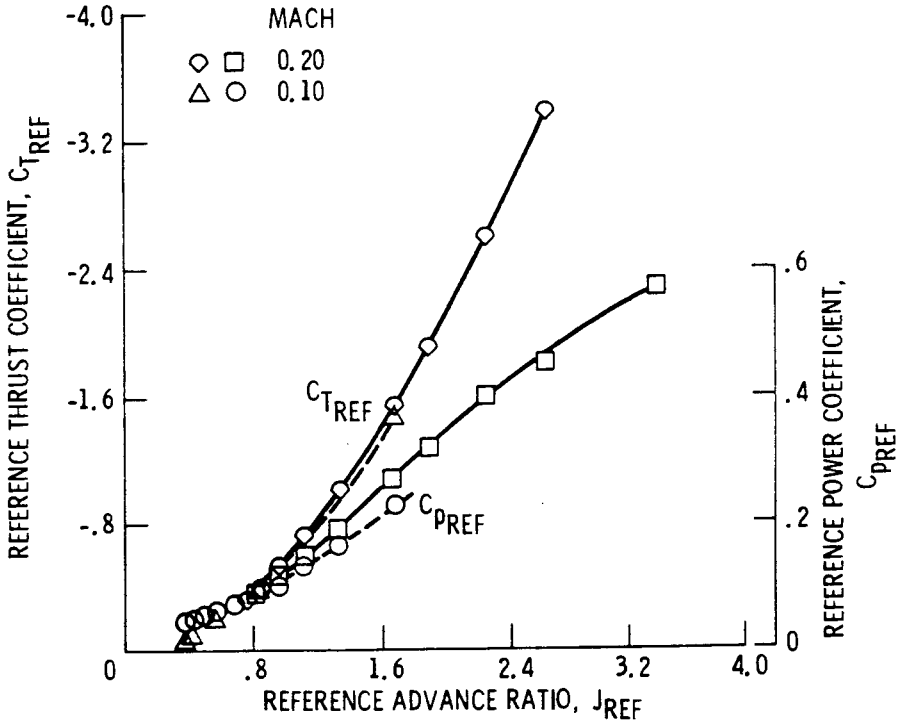

Figure 19. - SR-3 reverse thrust and power coefficients versus advance ratio for Mach numbers of 0.10 and 0.20. $\beta_{0.75R}$ = -6.8^0.

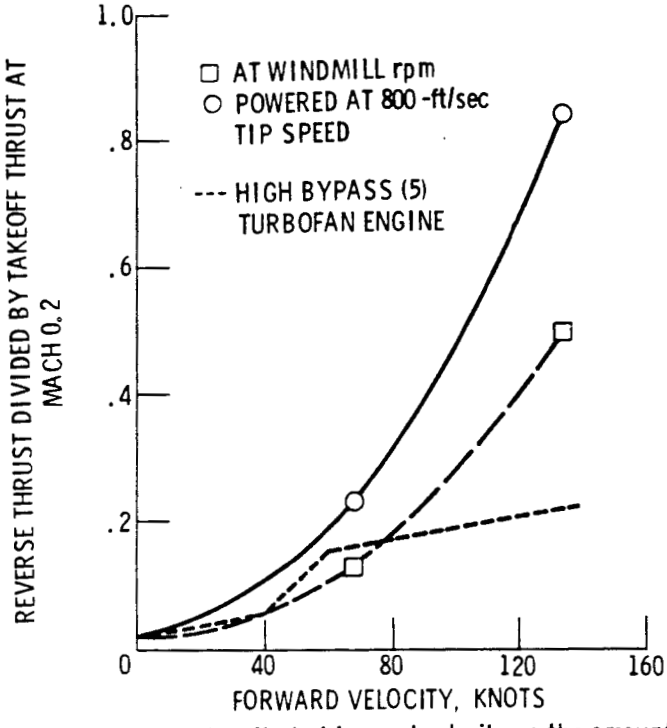

Figure 20. - The effect of forward velocity on the amount of reverse thrust produced relative to the amount of takeoff thrust produced at Mach 0.20. SR-3 propeller; $\beta_{0.75R} = -6.8^{0}$; takeoff thrust at $M_0 = 0.2$ equals 321. lbf.

1. Report No.	2. Government Accession No.	3. Recipient's Catalog No.
NASA TM-87054 AIAA-85-1259		

4. Title and Subtitle	5. Report Date
Wind Tunnel Results of Advanced High Speed Propellers in the Takeoff, Climb, and Landing Operating Regimes	6. Performing Organization Code 505-45-58
7. Author(s) George L. Stefko and Robert J. Jeracki	8. Performing Organization Report No. E-2621
	10. Work Unit No.
9. Performing Organization Name and Address National Aeronautics and Space Administration Lewis Research Center Cleveland, Ohio 44135	11. Contract or Grant No.
	13. Type of Report and Period Covered Technical Memorandum
12. Sponsoring Agency Name and Address National Aeronautics and Space Administration Washington, D.C. 20546	14. Sponsoring Agency Code

15. Supplementary Notes

Prepared for the Twenty-first Joint Propulsion Conference, cosponsored by the AIAA, SAE, ASME, and ASEE, Monterey, California, July 8-10, 1985.

16. Abstract

Low speed wind tunnel performance tests of two advanced propellers have been completed at the NASA Lewis Research Center as part of the NASA Advanced Turboprop Program. The 62.2 cm (24.5 in) diameter adjustable pitch models were tested at Mach numbers typical of takeoff, initial climbout, and landing speeds (i.e., from 0.10 to 0.34) in the NASA Lewis 10- by 10-Ft Supersonic Wind Tunnel. Both models had eight blades and a cruise design point operating condition of 0.80 Mach number, 10.668 km (35 000 ft) I.S.A. altitude, 243.8 m/s (800 ft/sec) tip speed and a high power loading of 301 kW/m^2 (37.5 shp/ft^2). No adverse or unusual low speed operating conditions were found during the test with either the straight blade SR-2 or the 45° swept SR-3 propellers. The 45° swept propeller efficiency exceeded the straight blade efficiency by 4 to 5 percent. Typical net efficiencies of the straight and 45° swept propeller at a Mach 0.20 takeoff condition were 50.2 and 54.9 percent respectively. At a Mach 0.34 climb condition, the efficiencies were 53.7 and 59.1 percent. Reverse thrust data indicated that these propellers are capable of producing more reverse thrust at Mach 0.20 than a high-bypass turbofan engine at Mach 0.20.

17. Key Words (Suggested by Author(s))	18. Distribution Statement
Propellers; Advanced turboprop; Energy efficient; Prop-fan	Unclassified - unlimited STAR Category 02

19. Security Classif. (of this report)	20. Security Classif. (of this page)	21. No. of pages	22. Price*
Unclassified	Unclassified		

*For sale by the National Technical Information Service, Springfield, Virginia 22161